

Nanosized Titania Composites for Reinforcement of Photocatalysis and Photoelectrocatalysis

Nanosized Titania Composites for Reinforcement of Photocatalysis and Photoelectrocatalysis

By

Maksym Zahornyi and Georgii Sokolsky

**Cambridge
Scholars
Publishing**



Nanosized Titania Composites for Reinforcement of Photocatalysis
and Photoelectrocatalysis

By Maksym Zahornyi and Georgii Sokolsky

This book first published 2022

Cambridge Scholars Publishing

Lady Stephenson Library, Newcastle upon Tyne, NE6 2PA, UK

British Library Cataloguing in Publication Data

A catalogue record for this book is available from the British Library

Copyright © 2022 by Maksym Zahornyi and Georgii Sokolsky

All rights for this book reserved. No part of this book may be reproduced, stored in a retrieval system, or transmitted, in any form or by any means, electronic, mechanical, photocopying, recording or otherwise, without the prior permission of the copyright owner.

ISBN (10): 1-5275-7786-4

ISBN (13): 978-1-5275-7786-2

CONTENTS

Abstract	viii
Preface	ix
Acknowledgements	xiii
List of abbreviations and symbols	xiv
Introduction	xvi
1. Titanium Dioxide Production, Properties, and Applications:	
A Brief Overview	1
1.1 Occurrence in Nature	1
1.2 Production Methods	3
1.3 Physical and Thermodynamic Properties	4
1.4 The metastability of TiO ₂	5
1.5 TiO ₂ Nanoparticle Safety Evaluation. Risks, Toxicity, and Application	6
1.6 TiO ₂ Synthesis	9
2. Photocatalytic Applications of TiO ₂ Nanoparticles: Inactivation of Pathogenic Microorganisms and Degradation of Dyes	15
2.1 Defects in Titanium Dioxide as Catalytic Doping Centre	15
2.2 TiO ₂ Nanoparticle Antimicrobial and Antiviral Activity	20
2.2.1 The following problems were found in a review of the literature	26
2.2.2 Experimental results and antiadenovirus activity of TiO ₂ nanoparticles	26
2.2.3 Materials and methods. Transplanted cell cultures used in the research	27
2.2.4 Influence of UV action with dose intensity on bacterial inactivation	29
2.2.5 The influence of irradiation intensity on bacterial inactivation	31

2.3 The Application of TiO ₂ in Photocatalysis	35
2.3.1 Spectral analysis of TiO ₂ nanoparticles.....	35
2.3.2 Oxidative destruction of dyes with TiO ₂	39
2.3.3 Nanophotocatalysis involving semiconductors of different natures.....	41
3. Preparation, Physicochemical Properties, and Application of Polymer Nanocomposites Filled with Oxide Nanoparticles.....	44
3.1 Synthesis, Molecular Structure, and Properties of C ₃ N ₄	44
3.1.1 The nature of the precursor influences C ₃ N ₄ surface structure and properties: Molecular structure of C ₃ N ₄	45
3.1.2 The temperature of precursor decomposition.....	48
3.1.3 Catalysis of C ₃ N ₄ systems	54
3.2 Progress in the Preparation and Application of Polyaniline.....	61
3.2.1 Molecular structure of polyaniline	63
3.2.2 The kinetics of oxidative polymerization and morphology of reaction products	66
3.2.3 Managed self-assembly and self-organization of polymer layers on the carrier	70
3.2.4 Mechanism of polymerization.....	74
3.2.5 The influence of pH on monomer polymerization	75
3.2.6 Spectral analysis of synthesized PANI.....	83
3.2.7 Conductivity and photocatalytic activity of polyaniline....	86
3.2.8 MXene functionalized polyaniline systems.....	89
3.3. Functional Composites with Different Types of Polymer Matrix ..	93
3.3.1 Polyaniline composites filled with metallic and oxide nanoparticles	93
3.3.2 Preparation methods and properties of organic composites with TiO ₂ nanoparticles	99
3.3.3 Polyacrylate composites with oxide nanoparticles.....	103
3.3.4 Synthesis and properties of polypyrrole nanostructures: optimization and applications	106
3.3.5 Some aspects of the oxidative polymerization of pyrrole by APS.....	107
3.3.6 Morphology and properties of polypyrrole nanocomposites.....	112
3.3.7 Pyrolysed metal-nitrogen-carbon (Me-N-C) catalyst reduction of oxygen based on polypyrrole	118

4. The Preparation and Optical Absorption of Polyaniline-TiO ₂ (C ₃ N ₄ O _x) Nanocomposites for Photocatalysis	125
4.1 Synthesis and Morphology of TiO ₂ Nanocomposites	127
4.1.1 TiO ₂ surface structure system	128
4.2 Spectral Characterization of TiO ₂ Nanocomposites.....	130
4.3 Photocatalytic Activity Test.....	132
4.3.1 Mechanism of irradiation of PANI-TiO ₂ nanocomposites	135
4.3.2 Nanostructured optical composites of C ₃ N ₄ O _x -polyaniline and C ₃ N ₄ O _x -TiO ₂	136
4.3.3 Synthesis of nanosized composites based on an oxide semiconductor and metal	144
5. Nanosized TiO ₂ Composites in Photoelectrocatalysis.....	150
5.1 General Aspects	150
5.1.1 PEC phenomena at the semiconductor/electrolyte interface in TiO ₂	152
5.1.2 Advantages of nanostructured transition metal oxides in PEC	154
5.1.3 Bandgap engineering in TiO ₂	156
5.1.4 TiO ₂ doping strategies in PEC	157
5.2 Titanium Dioxide and other Titanium Compounds in PEC	159
5.2.1 Substoichiometric compounds of TiO ₂	159
5.2.2 TiO ₂ polymorphs	159
5.3 PEC Degradation of Organics Using Titanium Dioxide	161
5.3.1 PEC methyl orange degradation by TiO ₂ of different origins	162
5.4 TiO ₂ -MnO ₂ System in PEC Processes	178
5.4.1 Manganese dioxide: its occurrence, polymorphic structure, and chemical thermodynamics.....	179
5.4.2 Manganese dioxide non-stoichiometry as a primary advantage for PEC.....	185
5.4.3 Manganese dioxide applications.....	191
5.4.4 TiO ₂ -MnO ₂ applications in PEC processes	194
Summary	200
Glossary of Terms	204
Bibliography.....	211

ABSTRACT

Today, innovative technologies using organic-inorganic composite materials are driving rapid progress in the development of novel water purification technologies. The unique surface, optical, and catalytic properties of nanomaterials based on oxide nanoparticles with varied natures has found widespread application in wastewater treatment.

Nanosized titanium dioxide and its composites are the most promising photocatalytically active materials and this book gives an overview of their application in photocatalysis and photoelectrocatalysis. In light of the continuing COVID-19 global emergency, this monograph also discusses the antimicrobial and antiviral activity of TiO₂ nanoparticles. A number of semiconducting and bioactive catalysts based on conjugated polymers and TiO₂-MnO₂, which have a redox function in water purification, are introduced.

The aim of this monograph is to analyse the state-of-the-art in this rapidly developing research area. As such, the authors' original research data are presented and composites based on polyaniline, polypyrrole, and nanosized TiO₂ nanoparticles are investigated.

Keywords: nanomaterials, TiO₂, photocatalyst, photoelectrocatalysis, conducting polymer, PANI, PPy.

Codes: PNRD, PNNP, PNN, PH

PREFACE

Photocatalysis using nanomaterials is fast becoming an effective strategy for environmental remediation. The activity of semiconductor nanomaterials predetermines their photocatalytic performance. Numerous photocatalysts have been studied and the results presented in papers and patents, including UV, visible, and full-spectrum light response photocatalysts for the treatment of contaminants of emerging concern (organic dyes, pesticides, and pharmaceutical pollutants, etc.). The optimization principles for efficient photocatalysts concern their high light response, utilization ability, excellent physicochemical stability, low cost, and environmental friendliness (Sabu et al. 2018).

The following three issues need to be addressed in future studies of these photocatalysts: efficiency in fast recombination of photogenerated electron-hole pairs; limited visible light response; and low specific surface area. On the one hand, strategies for existing materials need to be investigated further; on the other, the synthesis of new photocatalysts is urgently needed. Furthermore, to optimize the treatment of contaminants, different processes can be combined, including the strategies of adsorption, photocatalysis, and electrophotocatalysis. Additionally, the study of the morphological architecture of photocatalysts and their properties has significance for the design of stable photoelectrocatalytic materials. Important aspects in the preparation of photocatalytic materials are presented in this book.

This book is composed of five chapters. The first chapter is devoted to titanium dioxide (TiO_2) nanoparticles and covers: their occurrence in nature; technologies of their synthesis; their physical and thermodynamic properties; and their application. Nanosized polymorphs have been shown to improve the photocatalytic activity of TiO_2 particles. The shift in their capacity to absorb light, from UV to the visible region, is presented along with the positive and negative effects of impurities introduced into the TiO_2 structure. The influence of doping elements on the optical and photocatalytic activity of TiO_2 is also presented. The second chapter covers the application of nanoparticles in the reinforcement of photoactive TiO_2 composites.

The third chapter describes the preparation, physicochemical properties, and applications of polyaniline- $\text{TiO}_2(\text{C}_3\text{N}_4)$ nanocomposites. We

demonstrate the structural features and optical properties of C_3N_4 semiconductor systems. Graphite-like carbon nitride ($g-C_3N_4$) shows high potential for biohazard removal and photoelectrocatalytic hydrogen generation. However, due to its bandgap of 2.7 eV, $g-C_3N_4$ utilizes solar light at a wavelength below 460 nm. The engineering strategies used to resolve these issues, such as doping with oxygen, are described in this chapter. We present the oxidative polymerization kinetics of monomers; the relationship between the parameters of synthesis; and the structure of the PANI polymer. The self-organization process of polyaniline nanoparticles on substrates is presented and the monomer polymerization mechanism is studied. Optimal polymer synthesis parameters, as well as the role of the oxidizing agent, are also described.

Analysis of the literature has demonstrated that nanosized TiO_2 , as an anatase polymorph, possesses high photoactivity; TiO_2 concentration has some influence on thermoplastic photodegradation too. Currently, there is only fragmentary information concerning the polymerization of aqueous solutions of methyl methacrylate. Acrylate oligomers and rubber-methacrylate solutions hold the promise of new composites produced in situ under the action of UV light. TiO_2 additives have an influence on the photopolymerization process. This growing body of knowledge is proving useful in the development of efficient and highly stable photocatalysts for the purification of pathogenic microorganisms from water and air.

Chapter 4 presents experimental results that have been discussed by the authors at forums in France and Portugal. PANI has been used to prepare $PANI-TiO_2(C_3N_4O_x)$ and TiO_2-Ag nanocomposite photocatalysts. The IR, Raman, SEM, and EPR techniques were used to elucidate the mechanism of electron interaction in $PANI-TiO_2$, TiO_2-Ag nanocomposites. These $PANI-TiO_2$ composites exhibit significantly higher photocatalytic activity than PANI in the degradation of an MB (methylene blue) aqueous solution under UV irradiation. The results of XRD and EPR analysis have confirmed the strong interaction between TiO_2 and PANI nanoparticles. The $PANI-TiO_2$ photocatalyst (anatase, anatase-rutile) demonstrates high efficiency in photocatalytic applications and investigation of the ultraviolet-visible (UV-vis) characteristics, elemental composition, and chromatography of $PANI-TiO_2$ nanocomposites has confirmed the physicochemical interactions between the polymer and TiO_2 nanoparticles. The high photocatalytic activity of $PANI-TiO_2$ is seen in the rapidity of phenol degradation under UV and visible light irradiation. Phenol degradation occurs in the first 10–20 min. with a constant rate of $k \cdot 10^{-2} - 3 \cdot 10^{-2} \text{ min}^{-1}$.

Current aspects of TiO₂ photoelectrocatalysis (PEC) are the focus of the Chapter 5. The role of PEC phenomena, depending on the TiO₂ composite semiconductor/electrolyte interface and the influence of TiO₂'s polymorphic nature and potential gradient, have all been studied and the results are presented here. Unlike with electrocatalysis, semiconductor electrodes based on TM oxides are among the best available PEC materials. They have the advantages of low price and environmental abundance. The different strategies for doping TiO₂ in PEC include “co-doping”. Amino azo-dye methyl orange (MO) degradation under UV irradiation is also discussed in terms of the Ti³⁺ self-doping effect.

This book will be of use for students in areas closely oriented to materials science, chemistry, physics, and biology, as well as also for virologists and specialists in environmental pollution.

The authors have focused on semiconducting nanosized TiO₂ and its composites for the following reasons:

1. The TiO₂ semiconductor is stable in a wide pH range of 0 to 14.
2. Alongside its geometric-morphological and dimensional effects, its quantum-dimensional ones are also important because of the Mott-Wannier exciton radius, which can vary in the range of 0.8–1.9 nm depending on the size of the crystallite TiO₂.
3. The migration time (τ_{migr}) of photogenerated charges from the bulk of the particles to the surface is short (10 ps) compared to the time (τ_{rec}) of electron-hole recombination (100 ns).
4. The electron transfer time to the adsorbed substrates occurs in the range 50–200 picoseconds.
5. Being excellent oxidizing agents, photogenerated holes can mineralize organic pollutants directly. Additionally, the holes (h⁺) can also form hydroxyl radicals ($\bullet\text{OH}$) with strong oxidizing properties. Photoexcited electrons, on the other hand, can produce superoxide radicals ($\text{O}_2\bullet^-$) and $\bullet\text{OH}$. These free radicals and e⁻/h⁺ pairs are highly reactive and can induce a series of redox reactions. In terms of water splitting, photogenerated electrons are captured by H⁺ in water to generate hydrogen, while holes will oxidize H₂O to form O₂.
6. The TiO₂ photocatalyst has been widely used in the fields of renewable energy and environmental clean-up. However, the large bandgap of TiO₂, along with the fast recombination of charge carriers, significantly lowers its photocatalytic

performance. Studies of light absorption and charge recombination of doped TiO₂ particles are limited by the entangled parameters introduced in experimental conditions. Theoretical approaches have provided useful insights through the systematic modelling of TiO₂ particles.

7. The greatest challenge in PEC research is the development of stable semiconductor nanomaterials based on TiO₂ that are activated by solar radiation. This will lead to their application in the oxidation of organics, anion reduction, and CO₂ reduction, as well as in the electrosynthesis, disinfection, and generation of radicals through the photoelectrocatalytic process, which brings some particular issues. Noble metal nanoparticles combine both catalytic activity and chemical inertness in an electrolyte medium and usually display the best electrocatalytic performance; sometimes there are no alternatives.
8. The origin, dispersion, and particle shape of the material has a strong influence on the functional properties of non-stoichiometric oxides; this has stimulated our interest in new titanium dioxide preparation methods. Our aim is to study the activity of composite electrodes based on titanium dioxide of various origins and phase composition during photoelectrocatalytic degradation of MO under UV irradiation and then to analyze the efficiency of TiO₂ samples synthesized from domestically produced Ukrainian raw materials (in the form of a hydrated titanium dioxide TiO(OH)₂ suspension).

ACKNOWLEDGEMENTS

We would like to acknowledge the engineers and scientists (depart. 48, 35, 58) of the institute, with whom we have been associated for 16 years and have published the results of our research.

The authors wish to express their gratitude to Patsui V., Lobunets T., Tyschenko N., Prof. Ragulya A., Tomila T., Ievtushenko A., Kasumov A., Lavrynenko O., Kornienko O., Bondarenko M., Silenko P. (Institute for Problems of Materials Science, IPMS), Prof. Strelchuk V., Yuhimchuk V. (V.Ye. Lashkarev Institute of Semiconductor Physics, NASU), Prof. Christophe Colbeau-Justin, PhD. Ghazzal M.N., Teseer Bahry, Prof. H. Remita of Laboratory photocatalysis at Université Paris-Sud.

Some experiments and efforts would have been almost impossible without the valuable support of Prof. Ivanov S. (National Academy of Culture and Art Management, Kyiv, Ukraine), Prof. Ivanova N. (Institute of General and Inorganic Chemistry of NASU), and postgraduate students L. Zudina and N. Gayuk (National aviation university, Kyiv, Ukraine).

The authors also wish to thank Pankivska Yu., Biliavska L., Povnitsa O., Zahorodnia S. (Zabolotny Institute of Microbiology and Virology, NAS Ukraine) for the helpful anti-adenovirus activity study of TiO₂ nanoparticles and NAS Ukraine “Development of innovative photocatalytic nanostructured materials based on ZnO and TiO₂” (528/IPM-11/20) and the nano-program “The development of photocatalytic nanocomposites for viral inactivation in the air” (№ 40/20-H) for supporting this book.

LIST OF ABBREVIATIONS AND SYMBOLS

NPs – nanoparticles
LED – light-emitting diode
APS – ammonium persulfate
An – aniline
CFU – colony forming unit
MB – methylene blue
SBM – surfactant binder modifier
MMA – methyl methacrylate
PMMA – polymethyl methacrylate
PANI – polyaniline
PPy – polypyrrole
PC – polyvinylchloride
DBSA – dodecylbenzenesulfonic acid
PAA – polyacrylic acid
DMF – N, N-dimethylformamide
Q – quinoid
Ox – oxidizer
EtOH – ethanol
h⁺ – holes
C – concentration
TGA – thermogravimetric analysis
LUMO – lowest unoccupied molecular orbital
CB – conductivity band
VB – valence band
n – refractive index
GO – graphene oxide
PA – polyacrylate
PVA – polyvinyl alcohol
CVD – chemical vapour deposition
ORR – oxygen reduction reaction
N-CPs – nitrogen-containing conjugated polymers
PEC – photoelectrocatalysis
EPC – electro-photocatalytic
AOP – advanced oxidation process
BDD – boron doped diamond

BET – Brunauer-Emmett-Teller (method)
CBD – chemical bath deposition process
CMD – chemically synthesized MnO₂
CVA – cyclic voltammetry
DSA – dimensional stable anode
EDX – energy-dispersive X-ray spectroscopy
EMD – electrochemically obtained MnO₂
HRTEM – high resolution transmission microscopy (study)
ITO – indium-doped tin oxide
LAB – Lithium-air battery
LPD – liquid phase deposition
MCE – mineralization current efficiency
MO – methyl orange
MS – molecular sieves
NP – nanoparticle
NTAs – nanotube arrays
NT – nanotube
OER – oxygen evolution reactions
OMS – octahedral molecular sieves
ORR – oxygen reduction reaction
PJSC – Private Joint Stock Company
PTFE – polytetrafluoroethylene (emulsion)
PV – photovoltaic
PC – photocatalysis (photocatalytic)
RhB – Rhodamine B
SCE – standard calomel electrode
SEM – scanning electronic microscopy
SHE – standard hydrogen electrode
STH – solar-to-hydrogen efficiency
TA – terephthalic acid
TAOH – 2-hydroxyterephthalic acid
TM – transition metal
TMO – transition metal oxide
XPS – X-ray photoelectron spectroscopy
XRD – X-ray diffraction
VSM – vibrating sample magnetometer
WOCs – water oxidation cocatalysts

INTRODUCTION

Novel nanoscale composite materials with a polymer matrix are fast becoming an essential part of meeting current and future needs for clean water and air. The unique properties of nanomaterials and their convergence with current treatment technologies present great opportunities to revolutionize wastewater treatment (Sabu et al. 2018).

Semiconductor photocatalytic (PC) and electrophotocatalytic (EPC) technologies have been the object of many research efforts due to their applications in the fields of renewable energy and environmental protection and remediation. A number of studies have been devoted to the development of highly-efficient PC and EPC systems and the exploration of the fundamental parameters that can modify their performance. Semiconductors, such as TiO_2 , ZnO , and C_3N_4 , have proved to be excellent photocatalysts, capable of the absorption of natural sunlight as nanomaterials. The fast recombination rate of photogenerated electrons and holes has led to the utilization of green solar energy and a reduction in photocatalytic activity.

Titanium dioxide photocatalysis is a physicochemical process used in water and wastewater treatment. Its potential for advanced oxidation and disinfection of refractory pollutants and resistant pathogens has been highlighted in many works over the last 30 years. TiO_2 displays numerous benefits, such as low cost, durability, photostability, and non-toxicity. The most challenging issues concern how the heterogeneous phase of photocatalysts make it difficult to describe the physicochemical processes involved and the low yields for other established advanced oxidation processes needed for the development of technological applications at full-scale.

Nowadays, different methods, including shape, size, and facet control, and element doping have been developed to enhance photocatalytic performance by increasing their capacity for broad absorption of sunlight, prolonging the lifetime of photoinduced carriers, and enhancing photocatalytic stability. For example, greater efficiency has been achieved through shape control; doping with metal or non-metal elements; dye-sensitization; and the construction of heterostructured photocatalyst systems by combining them with novel plasmonic metals (i.e. Ag, Au, Pd, and Pt) or other semiconductors with polymers. Among these, the construction of

plasmonic metal-semiconductor heterojunctions is an effective strategy due to the effects of surface plasmon resonance (SPR) and Schottky junctions, which endow the heterojunction with the desirable properties. Noble metal nanoparticles (NPs) can show SPR, which can be tailored by engineering the shape, size, and surroundings. Therefore, noble metal NPs do not only strongly absorb visible light, but can also serve as electron sinks and as a source of active reaction sites. Accordingly, under irradiation with light, the photogenerated electron-hole pairs can be separated and the carriers can be transported efficiently at the interfaces of the metal-semiconductor. Over the last few years, one of the most closely investigated types of plasmonic metal-semiconductor heterostructured photocatalyst is a semiconductor decorated with plasmonic metal nanoparticles. The metal nanoparticles on the outside are exposed to the reactants and the surrounding medium, leading to corrosion and detachment from the semiconductor photocatalyst. An alternative option is to construct core-shell metal-semiconductor structures. As an important type of photocatalyst, one-dimensional (1D) semiconductor nanostructures and their hybrids with metal, as well as conducting polymer heterostructures, have been intensively explored (Sabu et al. 2018).

Morphology-controlled rutile titanium (IV) oxide (TiO_2) and anatase TiO_2 are prepared by the hydrothermal method and their surfaces are selectively loaded with Au, Ag, and Au-Ag bimetallic nanoparticles (NPs) through photodeposition to obtain visible light-responsive photocatalysts. With the help of local surface plasmon resonance (LSPR) noble metal NPs, the photocatalytic activity of noble metal-loaded TiO_2 under visible-light irradiation has been improved compared to that of bare TiO_2 . The enhancement of LSPR on the photocatalytic activity of rutile TiO_2 has been shown to be larger than that of anatase TiO_2 with an optimum amount of Au or Au-Ag. In addition, the reusability (stability) of Au-Ag-loaded TiO_2 has been shown to be much better than that of Ag-loaded TiO_2 . Double-beam photoacoustic results have confirmed how different trap energy level distributions lead to different electron transfer ways, resulting in different oxidizing capabilities; this presents an important strategy in the design of visible-light responsive TiO_2 (Zheng and Murakamia 2020).

The synthesis of 1D nanostructures and their potential applications in solar energy conversion has attracted much recent interest because of their unique 1D geometry with fast and long-distance electron transfer, good electron conductivity and mobility, large specific surface area, high light-harvesting efficiency, favourable length-to-diameter ratios, and high adsorption capacity. Taking into account the shortcomings of single component nanomaterials, such as ineffective utilization of visible light, low

quantum efficiency, and poor stability during photocatalysis, multicomponent 1D-based nano hybrids are expected to overcome such drawbacks and, accordingly, are being studied for heterogeneous photocatalysis.

The PEC process has the advantages of simplicity, rapidity, and controllable transformation inherent to electrochemical methods with a further rate increase due to catalytic effects on electrode materials in the presence of solar radiation. Pioneering work (Fujishima and Honda 1972, 238) on the discovery of TiO_2 PEC water splitting has been the cornerstone of this phenomenon, particularly for green and sustainable hydrogen production. Various applications of PEC technologies have been introduced in wastewater treatment.

CHAPTER 1

TITANIUM DIOXIDE PRODUCTION, PROPERTIES, AND APPLICATIONS: A BRIEF OVERVIEW

The development of nanotechnology has led to tremendous growth in the application of NPs for drug delivery systems, antibacterial materials, cosmetics, sunscreens, and electronics. In October 2011, the European Union defined nanomaterials as natural, incidental, or manufactured materials containing particles in an unbound state or as an aggregate or agglomerate, and where 50 % or more of the particles exhibit one or more external dimensions in the size range of 1–100 nm. Others have defined NPs as objects with at least one of their three dimensions in the range of 1–100 nm. NPs possess dramatically different physicochemical properties compared to fine particles of the same composition. The small size of NPs ensures that a large portion of atoms will be on the particle surface. Since surface properties, such as energy level, electronic structure, and reactivity are different from interior states, the bioactivity of NPs differs from that of fine size analogues (Shi and Magaye 2013, 15).

1.1 Occurrence in Nature

Pure TiO_2 is a colourless crystalline solid powder. Despite being colourless, in large quantities, if it is well cleaned, titanium dioxide is a white pigment. TiO_2 does not absorb incident light in the visible spectrum and so light is either transmitted or refracted through a crystal or reflected on to surfaces. TiO_2 is a stable, non-volatile substance that is insoluble in acids, alkalis, and solutions under normal conditions. Titanium dioxide is highly reactive to various compounds, including toxic ones contained in the air. Due to its inertness, titanium dioxide is non-toxic and, in general, is considered a very safe substance. TiO_2 does not dissolve in water, or in dilute mineral acids (except hydrofluoric acid) and dilute alkali solutions.

Our company, Nanotechcenter LLC (IPMS NASU), produces anatase of 10–20 nm (fig. 1.1) with the ability to absorb light in the UV

region (<http://ntc.co.ua/en/>). In its pure form, TiO_2 is found in nature in the form of the minerals rutile, anatase, and brookite (the first two are tetragonal in structure and the last is a rhombic phase), with rutile constituting the main part. The third-largest rutile deposit in the world is located in Rasskazovsky district in the Tambov region. Large deposits are also located in Chile (Cerro Bianco) and the Canadian province of Quebec (Woodruff and Bedinger 2017, 1802).

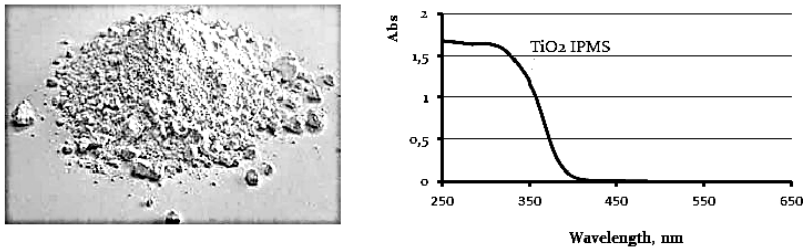


Fig. 1.1 The spectrum optical absorbance of TiO_2 (IPMS NASU).

Titanium-oxide minerals are denser than quartz and are left behind during erosion and weathering as lighter minerals are more rapidly transported away or broken down. Typical mineral assemblages in heavy-mineral deposits can include rutile and ilmenite (and minerals produced from the weathering of ilmenite, such as anatase, leucosene, and pseudorutile), as well as other high-density, erosion-resistant minerals, such as chromite, garnet, kyanite, monazite, staurolite, tourmaline, and zircon. Heavy-mineral deposits develop when relatively resistant iron-titanium-oxide minerals and other heavy minerals, such as monazite and zircon, are eroded from the parent rocks, transported and sorted, and finally deposited in fluvial (alluvial) settings. Many productive heavy-mineral locations, such as the east coast of the United States, the east and west coasts of South Africa, and the east and west coasts of Australia, are located on passive continental margins backed by elevated and metamorphic or mafic igneous hinterlands (Force 1991, 259).

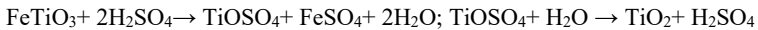
Titanium is the ninth most abundant element in the earth's crust, with an average TiO_2 abundance of 0.7 weight percent (wt%) (Rudnick and Fountain 1995, 3). Titanium can be found in nearly all rocks and sediments at more than one percent. Thus, unlike many other elements of economic interest, it is considered to be a major element rather than a trace element. Titanium is a transition element with the atomic number 22 and atomic mass of 47.867 atomic mass units. Titanium's chemistry shows

similarities to those of silicon and zirconium. The main oxidation state is Ti^{4+} , although Ti^{2+} and Ti^{3+} exist too. Titanium is a lithophilic element with a strong affinity for oxygen and it typically forms oxide minerals. It is not found as a pure metal in nature. Titanium metal is a high-strength metal with low density—as strong as steel but 45 percent lighter—and has excellent corrosion resistance.

1.2 Production Methods

Pigment TiO_2 is produced from titanium-containing concentrates using chloride and sulfate methods. In the chloride method, rutile is converted to titanium tetrachloride ($TiCl_4$) by chlorination in the presence of petroleum coke. In the sulfate process (48 % of world production capacity), ilmenite concentrates or titanium slag is decomposed by sulfuric acid. Precursor $TiCl_4$ is hydrolysed to hydroxide in the liquid phase with heat treatment of the precipitate by hydrolysis in water vapour, or burning in a stream of oxygen.

The sulfate method was developed in 1931, starting with the release of the anatase form of TiO_2 and followed by the synthesis of rutile in 1941. With this technology, an ore containing titanium is dissolved in sulfuric acid to form a solution of titanium sulfates, iron, and other metals. Then, as a result of a sequence of operations including chemical reduction, purification, precipitation, washing, and calcination, intermediate pigment-sized TiO_2 fractions are obtained.



DuPont developed and implemented the chloride method in 1948. Under reducing conditions, titanium ore interacts with gaseous chlorine to produce titanium chloride and other metal bichlorides, which are then separated. Subsequently, the finely purified $TiCl_4$ is oxidized at high temperatures to obtain high brightness intermediate titanium dioxide. At the oxidation stage, as part of the chlorination process, it is possible to tightly control the particle size distribution, as well as the type of crystal, making it possible to obtain titanium dioxide with excellent hiding and whitening properties.



In both technological processes, the sulfate and chloride methods give intermediates with TiO_2 crystal congestion and are separated (crushed) to obtain optimal optical characteristics. Depending on the end-user requirements, various processing methods are used to modify TiO_2 , including deposition of silicon, aluminium, zirconium, or zinc oxides on the surface of pigment fractions. Oxide treatment methods can be used in an aqueous or anhydrous medium to optimise performance for specific applications. Additionally, organic additives can be used to improve individual pigment characteristics.

Our laboratory obtained the titanium dioxide required for experimentation through the thermal decomposition of a precursor. The raw material was a suspension of hydrated titanium dioxide $\text{TiO}(\text{OH})_2$ (metatitanic acid)—a product of titanium concentrates and slags from “Sumykhimprom” (a Ukrainian company). The suspension was heated to $600\text{ }^\circ\text{C}$ with a heating rate of $5\text{ }^\circ\text{C}/\text{min}$ to obtain anatase. This production method promotes the formation of additional active centres on the surface of the TiO_2 . This process improves the optical and photocatalytic properties of anatase (<https://doi.org/10.15421/081914>).

A critical part of the production of TiO_2 is the supply of titanium ore. Titanium is one of the ten most common chemical elements on Earth and it is necessary to introduce rational methods for the extraction and enrichment of this mineral.

1.3 Physical and Thermodynamic Properties

Hydrated $\text{TiO}_2 \cdot n\text{H}_2\text{O}$ dioxide (titanium (IV) hydroxide), depending on the preparation conditions, may contain various numbers of OH groups bound to Ti, structural water, acid residues, and adsorbed cations. Freshly precipitated $\text{TiO}_2 \cdot n\text{H}_2\text{O}$ obtained in the cold is highly soluble in dilute mineral and strong organic acids, but insoluble in alkali solutions. It easily peptized with the formation of stable colloidal solutions. After the drying process, it forms a voluminous white powder with a density of $2.6\text{ g}/\text{cm}^3$ and a composition formula of $\text{TiO}_2 \cdot 2\text{H}_2\text{O}$ (acid). When heated, and with prolonged drying in a vacuum, it is gradually dehydrated, approaching the formula $\text{TiO}_2 \cdot \text{H}_2\text{O}$ (metatitanic acid). This powder is obtained through precipitation from hot solutions using the interaction of titanium metal with HNO_3 acid. The density of the powder is $\sim 3.2\text{ g}/\text{cm}^3$ or more. As they age, $\text{TiO}_2 \cdot n\text{H}_2\text{O}$ precipitates gradually turn into anhydrous dioxide, which keeps adsorbed cations and anions bound. The maturation of the powder is accelerated by the boiling water suspension. The structure of TiO_2 formed during aging is determined by the deposition conditions.

When the powder precipitates in acid solutions of pH <2, samples of anatase are formed

(http://www.plasma.com.ua/chemistry/chemistry/dioxid_titana.html).

The melting point of rutile is 1870 °C (according to other sources: 1850 °C and 1855 °C). The boiling point for rutile is 2500 °C and its density is 4.235 g/cm³. For anatase this is 4.05 g/cm³ (3.95 g/cm³), while for brookite it is 4.1 g/cm³. The decomposition temperature for rutile is 2900 °C. The melting, boiling, and decomposition temperatures for other modifications are not presented, because they become rutile after heating (see above).

Table 1.1 Average isobaric heat capacity C_p (J·mol⁻¹·K⁻¹)

type	Temperature interval, K					
	298-500	298-600	298-700	298-800	298-900	298-1000
rutile	60.71	62.39	63.76	64.92	65.95	66.89
anatase	63.21	65.18	66.59	67.64	68.47	69.12

Table 1.2 Thermodynamic properties

type	$\Delta H_{f,298}^{\circ}$, kJ·mol ⁻¹	$\Delta G_{f,298}^{\circ}$, kJ·mol ⁻¹	$C_{p,298}^{\circ}$, J·mol ⁻¹ ·K ⁻¹
rutile	-944.75 (-943.9)	-889.49 (-888.6)	55.04 (55.02)
anatase	-933.03 (-938.6)	-877.65 (-888.3)	55.21 (55.48)

Anatase is mainly stable at low temperatures, while the rutile phase is stable at high temperatures (tables 1.1 and 1.2). The Gibbs free energy of the anatase phase is lower than that of the rutile phase; TiO₂ initially prefers to nucleate into the anatase phase rather than into rutile. The phase transformation (anatase-rutile) is controlled by the annealing temperature, anatase nanocrystallites, and grain boundary defects (Choudhury 2013, 3). The particle arrangement and packing also influence the thermal stability and phase transformation behaviour of TiO₂ nanoparticles.

The metastability of TiO₂

TiO₂ forms three crystalline polymorphs—rutile (tetragonal), anatase (tetragonal), and brookite (rhombohedral). Rutile displays thermostability, while anatase reveals a metastable state with brookite when heating (Sato and Nakashima 2013, 3). The pattern formation of TiO₂ metastable modifications at atmospheric pressure is currently insufficiently studied. Several models explaining the stabilization of metastable phases at low

temperatures have been developed. The approach in which the main factor determining the phase composition of TiO_2 is the size factor (the amount of excess surface energy) has become widespread and thus the thermodynamic analysis of TiO_2 phase stability is presented. Anatase is more stable than rutile when the crystallite size is lower than 14 nm. This trend is also extended to brookite. Apparently, in different situations, various mechanisms of stabilization of anatase or brookite at low temperatures prevail, or the action of these mechanisms appears. After rutile phase formation at low temperatures, the transition to anatase or brookite is absent (fig. 1.2).

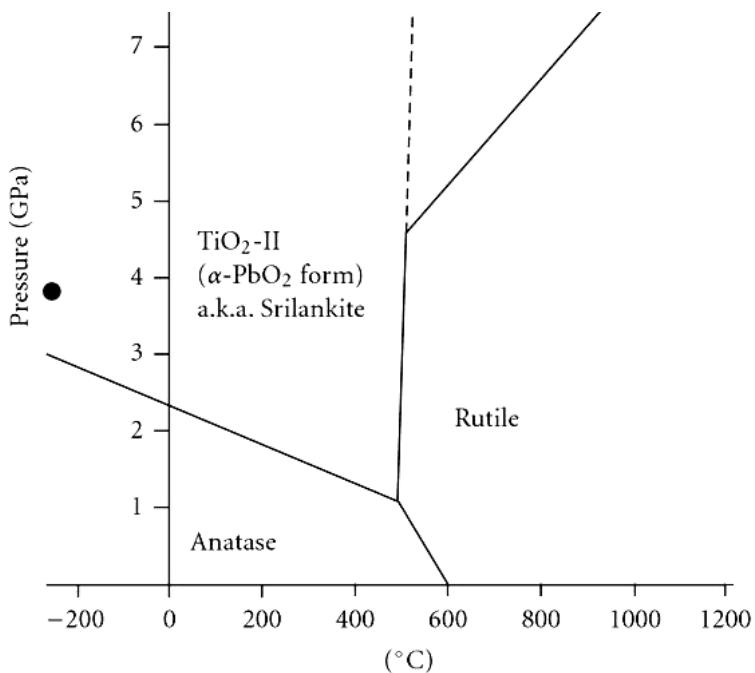


Fig. 1.2 Phase P-T diagram of TiO_2 .

1.4 TiO₂ Nanoparticle Safety Evaluation. Risks, Toxicity, and Application

Nanoparticles, nanotechnologies, and nanofabrication characterise the current stage of scientific and technological progress and are factors significantly influencing the further acceleration of this field (Yavorovsky and Tkachyshyn 2016, 3).

Nanoparticles and nanotechnologies have penetrated the fields of business, medicine, science, and even everyday life. On the one hand, these technologies allow us to obtain new materials, modified foods, and medicines, etc.; on the other they have potentially harmful and dangerous impacts on human health, the environment, and the biosphere as a whole (Zeinalov and Kombarova 2016, 3). Semiconductor NPs are characterised by special physicochemical properties that give them high reactivity and the ability to penetrate through biological barriers; as a consequence, they can affect the internal organs and systems of the body, causing pathological changes. The degree of toxicity of NPs depends on their chemical structure, shape, size, permeability, and surface area.

Proper toxicological evaluation of nanomaterials, as well as an understanding of the processes that occur on the surface of nanoparticles when in contact with living systems, is crucial to determining possible toxicological effects. The dose of the nanomaterials is important for identifying hazards and assessing the risks of using nanotechnologies (Zaroddu and Medici 2014, 33).

To date no standards have been developed for safe levels of nanomaterials in environmental objects in such areas as manufacturing, special workers' remedies, and methods for the safe handling of new materials based on nanostructures. As such, they should be handled with the utmost care as they are potentially dangerous to health (Demetska 2010, 4; Zavgorodnii and Dmuhovskaya 2013, 3). Here, the development of new toxicological approaches are required that consider the unique toxicity features of nanomaterials (Balbus and Maynard 2007, 11; Smith and Brown 2014, 2; Koivitsa and Kling 2017, 6).

According to the literature, a nanoparticle's toxicity is related to its: 1) chemical composition; 2) surface properties; 3) biotransformation products; and 4) development in terms of influence on apoptosis or necrosis of cells (Ghosh and Roy 2014, 6) or cell lysis (Simon and Saez 2017, 1). The mechanisms of toxicity are associated with oxidative stress, impaired mitochondrial function, and increased membrane permeability (Bosquet and Guaita-Esteruelas 2016, 249).

Scientists have determined lethal doses for nanoparticles in the form of solutions or oral suspensions (Wojcik and Sz wajgier 2019, 193). Toxicological studies of TiO₂ (20 nm) introduced to rats by inhalation have shown that particles with a size of 20 nm are capable of accumulating in lymphoid tissue (Ostiguy 2006, 52). They have been shown to have a damaging effect on the DNA of lymphocytes and brain cells (Jiang and Oberdörster 2008, 1). In mice, the LD50 of TiO₂ was found to be 1200 mg/kg and the long-term action of titanium dioxide led to the accumulation of nanoparticles in the brain, oxidative stress, excessive proliferation of glial cells, tissue necrosis, cell apoptosis, and neurogenic disease states (Ze and Hu 2014, 2).

The morphology and concentration of TiO₂ and ZnO nanoparticles leads them to significantly affect human organs. Exposure to fibre nanoparticles with a dose of 5–40 µg/ml results in cell death in the human bronchial epithelium. ZnO nanoparticles hold significant dangers because they are so widespread and are even found in antiseptic agents for children. Studies of *in vitro* toxicity of TiO₂, ZnO, and Al₂O₃ (30–47 nm) nanoparticles, used or proposed for use in some industries, suggest that ZnO has high toxicity, TiO₂ has moderate toxicity, and Al₂O₃ nanoparticles exhibit low toxicity at concentrations greater than 200 µg/ml (Zeinalov and Kombarova 2016, 3). The presence of ZnO nanoparticles (50 to 100 µg/ml) suppresses the mitochondrial function of Neuro-2A (murine neuroblastoma) cells. The relationship of organ-systemic toxicity to particle size may be due to the complex and often counter-directional dependencies between these sizes, the mechanisms of biological aggressiveness of the nanoparticles, and their toxicokinetics.

Analysis of the literature has allowed us to draw the following conclusions:

- Nanotechnologies, nanomaterials, and nanoparticles are seeing widespread use in various fields of economic activity, science, technology, medicine, and everyday life; however, there is a certain lag in biomedical research in assessing the risk of their impact on the human body.
- In the scientific literature, there is no unambiguous dependence shown in the protective and pathological reactions of organisms to the action of oxide semiconductor nanoparticles in terms of their particle size and nature.
- With decreasing size at the nanoscale, toxicity at the cellular level increases.

TiO₂ is used in the manufacture of fibreoptic products, medical equipment, and electronics. Titanium dioxide serves as a standard ingredient in ultrapure glass manufacture. It is also indispensable to the production of heat-resistant and optical glass and as a refractory protective coating for welding. In the manufacture of ceramics, titanium dioxide gives maximum whiteness to shards or enamels. Other areas of usage include: wood preservation (improving weather resistance by optical filtration of solar radiation); filling rubber; glass enamels; glass and glass ceramics; electroceramics; air purification; welding fluxes; hard alloys; chemical intermediates; and titanium dioxide-containing materials suitable for use at high temperatures (for example, fire protection in forced draft furnaces) and the analytical and experimental chromatography of liquids (Shi and Magaye 2013, 15).

Unfortunately, the process for obtaining TiO₂ nanomaterials (rods, tubes, and fibres) from the aqueous solution of precursor Ti(IV) is not well understood.

The technique used involves hydrothermal synthesis of titanium, zirconium, and hafnium dioxide at high-pressures of up to 4.0 GPa, which can give fundamentally novel results, revealing differences in the phase composition of hydrothermal treatment products as amorphous hydroxide gels and the solutions of corresponding compounds. It is interesting to study the process of obtaining one-dimensional (1D) nanostructures using titanium dioxide by the hydrothermal method, which should also lead to new results.

High temperatures in heat treatment allow us to increase the size of crystals, thereby reducing the number of surface defects of the material. This reduces the rate of recombination of electron pairs and promotes high photocatalytic activity. However, anatase can be transformed into the rutile phase and increasing the thermal stability of anatase is a priority task.

1.5 TiO₂ Synthesis

Titanium dioxide is a popular material with unique properties (Wang and Lin 2008, 20). Research has shown how the electrochemical anodizing of high-purity Ti foil allows the production of titanium dioxide membrane nanotubes with a high length to diameter ratio (approximately 1500). Anodizing occurred at room temperature and a platinum foil acted as a contoured electrode with a constant potential of 60 V. A membrane was formed of 135 μm thickness. The pore diameter, wall thickness, and length of the TiO₂ nanotubes were 90 nm, 15 nm, and 135 μm, respectively.

In another study, mesoporous titanium dioxide nanoparticles were synthesized by the aerosol-gel method (sol-gel) (Ahh and Cheou 2012, 188). Sodium chloride solutions (the amount of NaCl varying) in distilled water (90 ml) and titanium tetrabutoxide (17.15 ml) in ethanol (72.85 ml) were prepared separately. These solutions were combined and sonicated for 1 h. Next, the joint precursor was aerosolised, after being dried at 25 °C, and then nanostructured TiO₂-NaCl particles were formed at 500 °C, with sodium chloride acting as a template. The resulting TiO₂-NaCl composite nanoparticles were collected on a membrane filter and washed with deionized water using a centrifuge (3600 rpm for 10 min). The purification process was repeated twice to ensure complete removal of the NaCl. The specific surface area of the obtained nanoparticles was 286 and 184 m²/g, and the average pore size was 1.9 and 4.8 nm, respectively.

The synthesis of high-purity nanosized TiO₂ films by the sol-gel method has also been investigated (Sucio and Marian 2014, 384). Tetrabutoxy titanium (1 mmol) and propionic acid (1 mmol) were mixed for 3 h at 25 °C and part of the solution was used to obtain titanium dioxide in powder form. Heat treatment for 1 h at 450 °C led to the formation of TiO₂ with the structure of anatase and an average crystallite size of 17 nm. The second part of the solution was applied to ITO substrates (25x25 mm) by spin-coating (time 60 s, rotation speed 2000 rpm). The deposited layer was heated in the air for 2 h at a temperature of 450 °C. This gave a coating thickness of 72.33±20 nm and an average crystallite size of 11 nm.

A microemulsion was made consisting of cyclohexane (156 g), Triton X-100, hexanol (33 g), and hydrochloric acid (5 ml, 37 %). This mixture was used for TiO₂ nanoparticle synthesis (Khomane 2011, 1). After examination under a transmission electron microscope (TEM), the diameter of the synthesized particles was found to be 20–25 nm and the length exceeded 100 nm. The specific surface area was 135 m²/g and the average pore size was 10 nm.

Titanium dioxide nanoparticles can be in the form of one-dimensional structures (Wang and Li 2014, 19). Synthesis using the hydrothermal method (180 °C, 48 hours) yielded nanorods, needles, and smooth microspheres of titanium dioxide (Wei and Zang 2008). Due to the interaction of TiCl₄ with water, TiO₂ nanorods formed with a diameter of 60 nm and a length of 500–800 nm. FeCl₃ was added and needle microspheres formed with a diameter of 1–2 μm. Smooth microspheres formed only in the presence of the Span-80 surfactant and their size increased to 5–7 μm. In the X-ray diffraction patterns of both types of microspheres, the reflexes belonged to titanium dioxide with a rutile

structure, but anatase and brookite phases were also present. There were no crystalline phases containing iron in the X-ray diffraction patterns.

Use of the sol-gel method made it possible to obtain stable titanium dioxide fibres (You and Zhang 2012, 8) with a thickness of approximately 30 μm and a length of several metres. A solution of tetrabutoxy titanium in ethanol was prepared with a molar ratio of 1:3. This solution was slowly added dropwise to a solution of hydrochloric acid (6 mol/L) in water and absolute ethanol. After stirring for 2 h, it was heated in an oil bath at 110–140 $^{\circ}\text{C}$. From the colloidal solution (sol) obtained, fibres were pulled by blowing nitrogen. The crystallization of TiO_2 fibres was performed at 500 $^{\circ}\text{C}$ for 1.5 h. The best fibre formation was observed for a sol with the ratio $(\text{TiO}_2):n(\text{H}_2\text{O}) \leq 2$. The continuous fibres consisted of titanium dioxide with anatase and a rutile crystal lattice with a layered structure and an average particle size of 30 nm.

Titanium dioxide nanopowders were obtained by the hydrothermal method and the precipitation method at room temperature (El-Sherbiny and Fetma 2014). In the hydrothermal method, a TiO_2 ethanol solution was added dropwise to concentrated hydrochloric acid, diluted with water, and then subjected to intense stirring for 30 min. The mixture was placed in an autoclave, sealed, and heated to 120 $^{\circ}\text{C}$. The nanoparticles were a mixture of crystalline phases with anatase and brookite (100 $^{\circ}\text{C}$, 24 h), and a pure phase of anatase (120 $^{\circ}\text{C}$, 24 h), for which the average particle size was 6.2 nm. In the precipitation method, a tetrabutoxy titanium ethanol solution was added dropwise and stirred into a mixture of urea with hydrochloric acid at 0 $^{\circ}\text{C}$. After 4 h of stirring, the mixture was left for 2 weeks at 25 $^{\circ}\text{C}$. As a result, TiO_2 with a rutile structure was formed with an average particle size of 9.2 nm, confirmed by TEM analysis. Analysis showed that pure TiO_2 with an anatase structure had a specific surface area of 140.74 m^2/g and pore volume of 0.237 cm^3/g , while for TiO_2 with a rutile structure, these parameters were reduced to 60.621 m^2/g and 0.122 cm^3/g , respectively.

TiO_2 films were obtained by nonaqueous electrodeposition (Chigane and Shinagawa 2017). The source of titanium was orthotitanic acid n-hydrate ($\text{Ti}(\text{OH})_4 \cdot n\text{H}_2\text{O}$). Next, a galvanic solution consisting of titanium, electrolytes (tetramethylammonium chloride), and organic solvents (DMF and ethanol) were prepared. Glass (10x30 mm) was coated with a layer of titanium (20 nm thickness) and platinum (100 nm thickness) by spraying. A titanium plate was used as a counter electrode and a reference electrode. Films were deposited with a controlled potential of -1.8 V for 1 min. Then, the annealed electrodeposited samples were placed in a muffle furnace (600 $^{\circ}$

C, 1 h). Films of titanium dioxide with anatase structure were obtained with a thickness of 350 nm.

A rutile titanium dioxide powder (Amano and Nakata 2016, 14) was obtained by heating commercially-sourced P25 powder. The initial powder was a mixture of crystalline phases of TiO₂-anatase and rutile. This powder was heated at 300, 500, and 700 °C in a hydrogen atmosphere for 2 h at atmospheric pressure. The transition from anatase to rutile occurred after heating to 700 °C. At this temperature, the specific surface area decreased from 55 to 16 m²/g and the average crystallite size was 52 nm.

The conditions of hydrothermal synthesis and TiO₂ morphology were studied. A tetrabutoxy titanium (1 ml) solution was mixed with an aqueous solution of sodium hydroxide (60 ml, 0.2 M) containing 0.05 wt% hydrogen peroxide; following this, the solution was stirred (Tian and Luo 2016). Then, the solution was placed in an autoclave and heated to 180 °C, maintained for 24 h. The white product was washed in hydrochloric acid, deionized water, and acetone to clear the sodium cations. This process was followed by drying (70 °C, 24 h) and crystallization (400 °C, 1 h). The resulting particles had a spherical morphology. According to the results of SEM and TEM, the spheres consisted of various nano-objects of TiO₂. Nanoribbons formed after 2 h of heating and twisted nanosheets formed after 6 h of heating. Nanotubes formed after 18 and 24 h. X-ray diffraction patterns of the products confirmed the formation of TiO₂ with an anatase structure.

A restricting factor when using coatings with special properties is their low resistance to long-term operation. As such, a number of different approaches are used (Sakai and Kato 2016, 1). A hydrophobic coating was obtained using an epoxy resin to realize biomimetic self-healing abilities and titanium dioxide and fluoropolymer acted as the photocatalyst. A mixture of epoxy resin, amine, polyethylene glycol, titanium dioxide, and fluoropolymer particles was prepared. Stirring and heating were carried out to remove the amine and the mixture was washed to remove the polyethylene glycol before the powder was dried at 75 °C for 4 h. As a result, a super-hydrophobic surface was formed. This coating had high wear resistance—it retained its resistant properties after two years in the open air and for 6000 h with an accelerated atmospheric exposure test.

Pure titanium dioxide is not active in visible light. As such, a luminescent agent Er³⁺YAlO₃ was added to oxide nanoparticles to activate them (Wang and Li 2009, 4). Tetrabutoxy titanium provided the titanium source, acetic acid was used as the polymerization catalyst, and ethanol was the dispersion medium. A solution was prepared of tetrabutoxy